

Descriptive mineralogy. Numerous specimens from Ilha de Taquaral in the State of Minas Gerais, Brazil, have appeared on the dealer's market that show abundant large childrenite-eosphorite crystals and smaller amounts of wardite and a green botryoidal phase related to roscherite attractively grouped upon large rose quartz crystals and along joints and fractures in quartz and albite. Occasional specimens provide a pale tan to brown mineral occurring as bunched aggregates of small (1–5 mm) tabular crystals to large (up to 2 cm) thick tabular canoe-shaped individuals.

The paragenesis is interpreted as a moderate-temperature hydrothermal vein association where subordinate alkalis, alkaline earth, and transition metals and major aluminium and phosphate afforded a series of basic aluminium phosphates. It is likely that cations such as Fe^{2+} , Mn^{2+} , and Be^{2+} were derived from pre-existing primary phases, perhaps beryl and triphylite-lithiophilite, which were earlier attacked by the aqueous-rich fluid separate formed during core consolidation and their cations selectively leached and subsequently transported elsewhere to open fissures.

The new species, whiteite, is pale tan (the type) to chocolate brown (the Ca-poor variant) and nearly colourless in small fragments. The hardness is 3 to 4 and the cleavage is $\{001\}$ good to perfect. The specific gravity for the pale tan type is 2.58(1) and for the Ca-poor variant 2.67(2), both determinations made on the Berman torsion balance with toluene as the displaced fluid at 21 °C.

Crystal morphology. Both whiteite and its Ca-poor variant occur as warped crystals showing the forms $c\{001\}$ and $n\{\bar{1}11\}$. These crystals are invariably twinned by reflection on $\{001\}$, imparting a pseudo-orthorhombic appearance to the composite. For the type, $c\{001\}$ is very large and affords tabular crystals with a rhombus-shaped outline whose acute angle in the plan view is $50^\circ 04'$ (fig. 1). These crystals range from 1 to 5 mm in greatest dimension.

The Ca-poor variant consists of crystals up to 1.5 cm in length where the areas of $c\{001\}$ and $n\{\bar{1}11\}$ are nearly balanced, affording a canoe-shaped outline to the crystals. This appearance is made more pronounced by the curved aspect of the $n\{\bar{1}11\}$ facets resulting in an almond-shaped cross-section. The structural basis for twinning in the whiteites is advanced in the next section.

X-ray crystallography. Single crystals of type whiteite and its Ca-poor variant were studied by rotation, Weissenberg, and precession photography. In addition, crystals were ground with glass and powder diffractometer traces were obtained (1° min^{-1} in 2θ ; Cu- K_α radiation with graphite monochromator). Owing to relatively few strong

reflections and frequent near-coincidence of the planes, considerable difficulty was encountered in unambiguously indexing these data. To overcome the uncertainties of Miller index assignment, the strong single crystal intensities were used as a guide. This was achieved by utilizing the atomic coordinate parameters in Moore and Araki (1974a) from which calculated powder patterns could be directly obtained. This calculation was also done for the whiteite member by assuming perfect isomorphic replacement. Built into the least-squares programme is an option to correct for absorption effects; the observed data reported in Table I, however, constitute the initial input for these have most meaning in routine powder diffractometry as a determinative tool. The indexed powder data (Table I) were then used to obtain the single-crystal results (Table II) by least-squares refinement. These were in turn used to calculate the d -spacings. Of the possible single-crystal intensities, only about 10% are sufficiently strong to appear on diffractometer traces and, consequently, the powder patterns deceptively suggest a simple compound. Due to considerable overlap of intensities arising from non-equivalent planes, the least-squares convergences are not as precise as expected for a crystal structure of moderate complexity.

The single-crystal photographs clearly revealed the twinned character of both whiteite samples, and the photographs could be interpreted on the basis

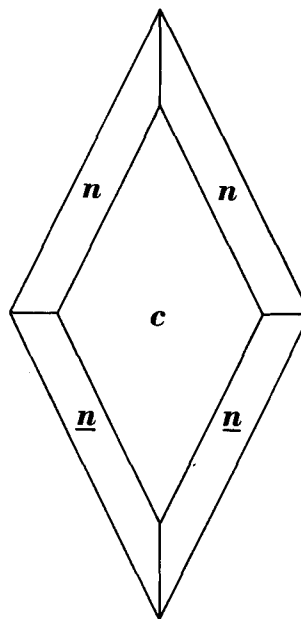


FIG. 1. Plan of whiteite twinned by reflection on $\{001\}$ showing the forms $c\{001\}$ and $n\{\bar{1}11\}$. Taquaral pegmatite.

of the jahnsite crystal structure reported by Moore and Araki (1974a). Define $c' = 2c + a/2$, and $\cos \beta' = [a/2]^2 - (c')^2 - (2c)^2 / ac'$. The pseudo-orthorhombic criteria are then a , b , c' , and β' , and Table II shows that β' is in the range $90 \pm 2^\circ$. Presumably, the closer β' is to orthogonality, the greater the likelihood of twinning.

Chemical composition. Both type whiteite and its calcium-poor variant were examined by electron-microprobe analysis, the refined results of which are presented in Table III as analyses 1a and 5. As in the jahnsite study of Moore (1974a), here repeated as analysis 6a, the oxide percentages are all slightly low and formula compositions are based on $P = 4$, that is, half the unit-cell contents. Since the structure type and atomic positions are known (Moore and Araki, 1974a), the problem reduces to a site distribution compatible with the general formula, $X M(1)M(2)_2 M(3)_2^3 + (OH)_2 (H_2O)_8 [PO_4]_4$, where X accommodates the largest cations such as Ca^{2+} , Mn^{2+} , minor Na^+ , etc.; $M(1)$ accommodates Mn^{2+} and Fe^{2+} ; $M(2)$ accommodates Mg^{2+} , Mn^{2+} , Fe^{2+} , and even Mn^{3+} and Fe^{3+} (for highly oxidized material); and $M(3)$ accepts Al^{3+} and Fe^{3+} . In this formula the M cations are in distorted octahedral coordination. In whiteites as in the jahnsites all water molecules and hydroxyl groups are bound to cations in the structure and are assumed to be quantitatively present. We propose the following distributions:

| | Whiteite (type) | Whiteite (Ca-poor) |
|--|-------------------------------|-------------------------------|
| X | $Ca_{0.9}^{2+} Mn_{0.1}^{2+}$ | $Mn_{0.8}^{2+} Ca_{0.2}^{2+}$ |
| $M(1)$ | $Fe_{0.7}^{2+} Mn_{0.3}^{2+}$ | $Fe_{0.9}^{2+} Mn_{0.1}^{2+}$ |
| $M(2)$ | $Mg_{1.0}^{2+}$ | $Mg_{1.0}^{2+}$ |
| $M(3)$ | $Al_{1.0}^{3+}$ | $Al_{1.0}^{3+}$ |
| ρ (calc., g cm ⁻³) | 2.51 | 2.62 |

It is tempting to suggest that the Ca-poor variant formed earlier and recovered the Mn^{2+} cations in solution. At a later stage, when nearly all Mn^{2+} was removed from the fluid, the Ca^{2+} -rich phase crystallized. This is consistent with the observation that the Ca-poor variant occurs as large crystals and its growth probably spanned a longer period of time.

As this paper was completed and ready for submission, Mr. Gunar Penikis of Toronto submitted three samples of tentatively identified whiteite from the Blow River, Yukon Territory, Canada, a locality that has become a source of unusual phosphate species and recently described by Mandarino and Sturman (1976). The specimens were sections of coarse crystals, tan to grey in colour and much resembling albite in appearance, and of sufficient quantity to warrant complete wet-chemical analyses. The results, given in Table III as

analyses 2, 3, and 4, confirm the general formula for the whiteite-jahnsite series and are in excellent agreement with theoretical cation contents in the formula unit. These three samples belong to whiteite—($CaFe^{2+}Mg$). A powder pattern from the sample used for analysis 2 is given in Table I and is in general agreement with type whiteite. Mr. Penikis informs us that the sample representing analysis 2 came from an 'A-vein', analysis 3 from a 'B-vein and found in 1974', and analysis 4 from a 'special type vein found two miles down from the main campsite in 1976 and associated with lustrous siderite and lazulite'. Since our specimens are only sections of crystals it is not possible to reconstruct the detailed paragenetic setting at these occurrences.

Optical data for the two whiteites and the jahnsites that have been studied in detail are summarized in Table IV.

Name. It is fitting to christen the new species after Mr. John S. White, Jr., Editor of *Mineralogical Record*, and Associate Curator of Minerals and Gems, the U.S. National Museum of Natural History. His liaison between amateur and professional communities has provided many examples of fine specimens for research that otherwise would have passed unnoticed and he has played a major role in the renaissance of mineralogy as an amateur as well as professional pursuit. The type specimens are preserved in the U.S. National Museum of Natural History collections.

The jahnsite-whiteite series: a proposed nomenclature

We propose that $M(3)$ distinguishes the jahnsites from the whiteites where $Fe^{3+} > Al^{3+}$ for the former and $Al^{3+} > Fe^{3+}$ for the latter. There is no evidence as yet that solid solution between the two is extensive—no such compositions have been found—but there is no structural reason to suspect why such solution could not exist.

Since the description of jahnsite by Moore (1974a), the species and its variants have been found at many pegmatite localities. It occurs as orange splinters intergrown with rockbridgeite, as brown warty aggregates, as yellow to greenish prismatic crystals either single or twinned and as granular orange masses. Recurrent crystal forms are $c\{001\}$, $a\{100\}$, $j\{201\}$, and $n\{\bar{1}11\}$. Unlike whiteite, jahnsite crystals are nearly always prismatic and striated parallel to $[010]$; thin tabular development has not been observed. It can be visually confounded with laueite, pseudolaueite, stewartite, childrenite, and the xanthoxenite of Frondel (1949). We have found a zero-level b -rotation axis Weissenberg photograph the most

TABLE I. *Whiteites and jahnsites. X-ray powder data*†

312

| 1 | | | 2 | | 3 | | | 4 | | | 5 | | | 6 | | 7 | | |
|-------------------------|--------------------------|------------|-------------------------|-------------------------|-------------------------|-------------------------|--------------------------|-------------------------|-------------------------|--------------------------|-------------------------|--------------------------|------------|-------------------------|-------------------------|-------------------------|-------------------------|--------------------------|
| <i>I/I</i> ₀ | <i>d</i> _{calc} | <i>hkl</i> | <i>I/I</i> ₀ | <i>d</i> _{obs} | <i>I/I</i> ₀ | <i>d</i> _{obs} | <i>d</i> _{calc} | <i>I/I</i> ₀ | <i>d</i> _{obs} | <i>d</i> _{calc} | <i>I/I</i> ₀ | <i>d</i> _{calc} | <i>hkl</i> | <i>I/I</i> ₀ | <i>d</i> _{obs} | <i>I/I</i> ₀ | <i>d</i> _{obs} | <i>d</i> _{calc} |
| 100 | 9.358 | 001* | 100 | 9.270 | 100 | 9.318 | 9.312 | 100 | 9.304 | 9.317 | 100 | 9.322 | 001* | 10 | 9.27 | 100 | 9.150 | 9.208 |
| 5 | 6.943 | 201 | 5 | 6.899 | | | | | | | | 1 | 7.140 | 010 | 1 | 7.08 | | |
| 2 | 6.920 | 010 | | | | | | | | | | 1 | 7.012 | 200 | | 10 | 6.897 | 6.997 |
| 2 | 6.859 | 200 | 5 | 6.805 | 5 | 6.920 | 6.883 | | | | 3 | 6.363 | 110 | 2 | 6.32 | | | |
| 5 | 6.178 | 110 | 5 | 6.189 | 5 | 6.214 | 6.211 | 3 | 6.230 | 6.220 | 11 | 5.686 | 111 | 4 | 5.66 | 5 | 5.639 | 5.697 |
| 19 | 5.621 | 111 | 35 | 5.563 | 30 | 5.598 | 5.654 | 15 | 5.593 | 5.659 | 7 | 5.003 | 210 | | 25 | 4.961 | 5.002 | |
| 3 | 4.901 | 211 | | | 20 | 4.922 | 4.894 | 15 | 4.924 | 4.890 | 17 | 4.910 | 111 | 6 | 4.91 | 15 | 4.844 | 4.876 |
| 13 | 4.872 | 210 | 30 | 4.901 | 50 | 4.824 | 4.787 | 20 | 4.849 | 4.793 | 11 | 4.661 | 002* | 4 | 4.63 | 40 | 4.602 | 4.604 |
| 30 | 4.790 | 111 | 65 | 4.822 | 40 | 4.644 | 4.656 | 30 | 4.660 | 4.658 | 7 | 4.076 | 112 | 3 | 4.05 | 10 | 4.059 | 4.063 |
| 8 | 4.679 | 002* | 65 | 4.637 | 20 | 4.036 | 4.093 | 10 | 4.043 | 4.095 | 8 | 3.911 | 310 | 3 | 3.90 | 10 | 3.887 | 3.907 |
| 9 | 4.084 | 112 | 20 | 4.022 | | | | | | | 1 | 3.733 | 401 | 1 | 3.723 | | | |
| 2 | 4.009 | 311 | | | | | | | | | 9 | 3.541 | 312 | 5 | 3.522 | 10 | 3.550 | 3.559 |
| 3 | 3.954 | 212 | | | 20 | 3.875 | 3.831 | 10 | 3.866 | 3.822 | 11 | 3.506 | 400 | | 30 | 3.483 | 3.498 | |
| 13 | 3.815 | 310 | 25 | 3.853 | 5 | 3.746 | 3.746 | 5 | 3.718 | 3.723 | 11 | 3.426 | 402 | 3 | 3.416 | 30 | 3.451 | 3.453 |
| 3 | 3.712 | 401 | 5 | 3.697 | 5 | 3.518 | 3.599 | 10 | 3.515 | 3.589 | 4 | 3.334 | 021 | | | | | |
| 16 | 3.567 | 312 | 35 | 3.498 | 30 | 3.454 | 3.510 | 15 | 3.487 | 3.490 | 7 | 3.284 | 311 | 3 | 3.268 | 5 | 3.247 | 3.259 |
| 12 | 3.472 | 402 | 40 | 3.476 | | | | | | | 2 | 3.181 | 220 | | | | | |
| 2 | 3.454 | 112 | | | | | | | | | 3 | 3.166 | 221 | 2 | 3.165 | 5 | 3.179 | 3.176 |
| 10 | 3.430 | 400 | 25 | 3.402 | | | | 10 | 3.421 | 3.426 | 18 | 2.962 | 401 | 5 | 2.950 | 15 | 2.925 | 2.936 |
| 1 | 3.245 | 021 | | | | | | | | | 12 | 2.867 | 403 | | 15 | 2.887 | 2.882 | |
| 11 | 3.194 | 311 | 30 | 3.246 | 35 | 3.245 | 3.191 | 10 | 3.257 | 3.188 | 47 | 2.834 | 022 | 8b | 2.825 | 55 | 2.808 | 2.825 |
| 3 | 3.119 | 003* | 25 | 3.094 | 8 | 3.094 | 3.104 | 10 | 3.107 | 3.106 | 16 | 2.580 | 421 | 4 | 2.575 | 15 | 2.581 | 2.589 |
| 2 | 3.073 | 410 | | | | | | | | | 2 | 2.428 | 402 | 2 | 2.417 | | | |
| 1 | 3.068 | 121 | | | | | | | | | 1 | 2.417 | 123 | | | | | |
| 3 | 2.992 | 212 | 10 | 3.026 | | | | | | | 3 | 2.349 | 404 | 3 | 2.341 | 10 | 2.339 | 2.354 |
| 16 | 2.933 | 403 | 70 | 2.941 | 45 | 2.948 | 2.960 | 20 | 2.946 | 2.948 | 2 | 2.341 | 611 | | | | | |
| 8 | 2.914 | 313 | | | | | | | | | 3 | 2.322 | 612 | | | 10 | 2.334 | 2.337 |
| 20 | 2.883 | 401 | 40 | 2.849 | 20 | 2.879 | 2.879 | 15 | 2.863 | 2.871 | 1 | 2.308 | 114 | 2 | 2.295 | 5 | 2.296 | 2.289 |
| 3 | 2.810 | 222 | | | | | | | | | 6 | 2.008 | 422 | 3 | 2.002 | | | |
| 3 | 2.794 | 221 | | | | | | | | | 2 | 2.007 | 403 | | | | | |
| 63 | 2.782 | 022 | 80 | 2.781 | 90 | 2.776 | 2.787 | 65 | 2.789 | 2.793 | 5 | 1.963 | 424 | | | | | |
| 2 | 2.675 | 312 | 5 | 2.643 | 5 | 2.678 | 2.702 | | | | 2 | 1.960 | 614 | 3 | 1.958 | 10 | 1.970 | 1.972 |
| 1 | 2.613 | 122 | 5 | 2.615 | 10 | 2.610 | 2.614 | | | | 9 | 1.951 | 024 | | | | | |
| 2 | 2.609 | 113 | 10 | 2.582 | 12 | 2.599 | 2.597 | 5 | 2.590 | 2.599 | 3 | 1.948 | 405 | 4 | 1.945 | 10 | 1.935 | 1.946 |
| 4 | 2.551 | 510 | | | | | | | | | 2 | 1.946 | 232 | | | | | |
| 19 | 2.531 | 421 | 30 | 2.535 | 25 | 2.544 | 2.549 | 20 | 2.542 | 2.546 | 9 | 1.866 | 802 | 4 | 1.870 | 20 | 1.874 | 1.876 |
| 2 | 2.502 | 203 | | | | | | | | | 6 | 1.785 | 040 | 2 | 1.787 | | | |
| 2 | 2.459 | 602 | | | | | | | | | 1 | 1.776 | 711 | 1 | 1.777 | | | |
| 2 | 2.413 | 223 | | | | | | | | | 2 | 1.750 | 423 | 2 | 1.746 | | | |
| 3 | 2.409 | 404 | 5 | 2.412 | 8 | 2.408 | 2.424 | | | | 2 | 1.713 | 804 | 2 | 1.712 | | | |
| 2 | 2.395 | 222 | | | | | | | | | 2 | 1.710 | 425 | | | | | |
| 1 | 2.368 | 402 | 5 | 2.381 | 8 | 2.380 | 2.357 | | | | 1 | 1.667 | 042 | 1 | 1.669 | | | |

P. B. MOORE AND J. ITO

TABLE II. *Whiteites and jahnsites. Single-crystal data*

| | 1 | 2 | 3 | 4 | 5 | 6 |
|-----------------------------------|---------------|---------------|--------------|--------------|---------------|-------|
| <i>a</i> (Å) | 14.90(4) | 14.85(5) | 14.99(2) | 14.94(2) | 15.01(3) | 15.02 |
| <i>b</i> (Å) | 6.98(2) | 6.92(4) | 6.96(1) | 7.14(1) | 7.15(2) | 7.23 |
| <i>c</i> (Å) | 10.13(2) | 10.13(4) | 10.14(1) | 9.93(1) | 9.87(2) | — |
| β | 113° 07'(10)' | 112° 30'(12)' | 113° 19'(6)' | 110° 10'(6)' | 111° 14'(10)' | — |
| <i>c'</i> (Å) | 18.64 | 18.72 | 18.63 | 18.65 | 18.42 | 18.75 |
| β' | 91° 33' | 91° 01' | 91° 36' | 88° 06' | 88° 55' | — |
| ρ (obs, g cm ⁻³) | 2.58 | — | 2.67 | 2.71 | 2.86 | 2.85 |

1. Type whiteite from Taquaral. Single-crystal study and resulting cell parameters refined from powder data. Space group *P2/a*.

2. Whiteite from Yukon. Cell parameters refined from powder data.

3. Ca-poor whiteite from Taquaral. Single-crystal study and resulting cell parameters refined from powder data. Space group *P2/a*.

4. Jahnsite (type). Data from Moore (1974). Space group *P2/a*.

5. Jahnsite from the Fletcher mine. Single-crystal study and resulting cell parameters refined from powder data. Space group *P2/a*.

6. Jahnsite from the Fletcher mine. Data from Mrose (1955). The space group was not stated.

TABLE III. *Whiteites and jahnsites. Chemical analyses**

| | 1 | | 2 | 3 | 4 | 5 | 6 | | 7 | | |
|--------------------------------|------|-------|-------|-------|-------|------|------|-------|------|-------|-------|
| | a | b | | | | | a | b | a | b | c |
| Na ₂ O | — | — | 0.17 | 0.32 | 0.28 | — | — | — | 0.4 | 0.51 | — |
| CaO | 6.0 | 6.7 | 5.98 | 3.80 | 3.57 | 1.4 | 6.6 | 6.9 | 2.6 | 3.27 | — |
| MgO | 10.5 | 10.6 | 12.55 | 11.32 | 9.99 | 10.1 | 9.4 | 9.9 | 2.7 | 3.39 | — |
| MnO | 3.1 | 3.7 | 0.45 | 0.28 | 2.18 | 7.6 | 8.0 | 8.7 | 10.2 | 12.84 | 23.9 |
| FeO | 6.1 | 6.6 | 9.57 | 12.62 | 11.80 | 7.9 | — | — | — | 7.97 | — |
| Al ₂ O ₃ | 12.0 | 13.5 | 11.54 | 11.42 | 11.62 | 12.7 | 2.1 | — | — | — | — |
| Mn ₂ O ₃ | — | — | — | — | — | — | — | — | — | — | — |
| Fe ₂ O ₃ | — | — | 0.25 | 0.60 | 1.14 | — | 15.1 | 19.6 | 22.8 | 19.95 | 26.9 |
| P ₂ O ₅ | 36.0 | 37.5 | 37.68 | 36.86 | 37.49 | 36.4 | 32.2 | 35.0 | 29.6 | 33.15 | 31.9 |
| H ₂ O(-) | — | 21.4 | 10.35 | 9.76 | 5.92 | — | 18.8 | 19.9 | — | 18.92 | 17.3 |
| H ₂ O(+) | — | | 11.21 | 11.55 | 15.87 | | | | | | |
| Total | 73.7 | 100.0 | 99.75 | 99.53 | 99.86 | 76.1 | 92.2 | 100.0 | 68.3 | 100.0 | 100.0 |

* Unless otherwise stated, the formula unit is expressed as $XM(1)M(2)_2M(3)_2(H_2O)_8(OH)_2(PO_4)_4$.

1a. Type whiteite from Brazil. A. J. Irving, analyst.

1b. Calculated composition for $X = Ca_{0.9}Mn_{0.1}^{2+}$; $M(1) = Fe_{0.7}^{2+}Mn_{0.3}^{2+}$; $M(2) = Mg_{1.0}$; $M(3) = Al_{1.0}$.

2. Yukon whiteite. J. Ito, analyst. This yields $X = Ca_{0.81}Fe_{0.09}^{2+}Mn_{0.05}^{2+}$; $M(1) = Fe_{0.92}^{2+}Mg_{0.08}$; $M(2) = Mg_{1.00}$; $M(3) = Al_{0.85}Mg_{0.14}Fe_{0.01}^{3+}$. Trace elements: K, Ba, Sr, Cr.

3. Yukon whiteite. J. Ito, analyst. This yields $X = Ca_{0.53}Fe_{0.34}^{2+}Na_{0.08}Mn_{0.03}^{2+}$; $M(1) = Fe_{1.00}^{2+}$; $M(2) = Mg_{0.99}Fe_{0.01}^{2+}$; $M(3) = Al_{0.87}Mg_{0.10}Fe_{0.03}^{3+}$. Total includes 1.40% SiO₂. Trace elements: Ba, Sr, Cr.

4. Yukon whiteite. J. Ito, analyst. This yields $X = Ca_{0.49}Mn_{0.24}Fe_{0.09}^{2+}Na_{0.07}$; $M(1) = Fe_{1.00}^{2+}$; $M(2) = Mg_{0.90}Fe_{0.10}^{2+}$; $M(3) = Al_{0.88}Mg_{0.06}Fe_{0.06}^{3+}$. Trace elements: Zn, Ba, Sr, Cr.

5. Whiteite, Ca-poor variant from Brazil. J. Nelen, analyst. This yields $X = Mn_{0.8}^{2+}Ca_{0.2}$; $M(1) = Fe_{0.9}^{2+}Mn_{0.1}^{2+}$; $M(2) = Mg_{1.0}$; $M(3) = Al_{1.0}$.

6a. Type jahnsite from Moore (1974).

6b. Calculated composition for $X = Ca_{1.0}$; $M(1) = Mn_{1.0}^{2+}$; $M(2) = Mg_{1.0}$; $M(3) = Fe_{1.0}^{3+}$.

7a. Jahnsite from the Fletcher mine. A. J. Irving, analyst.

7b. Calculated composition for $X = Ca_{0.50}Mn_{0.36}^{2+}Na_{0.14}$; $M(1) = Mn_{1.00}^{2+}$; $M(2) = Fe_{0.48}^{2+}Mg_{0.36}Mn_{0.10}^{2+}Fe_{0.06}^{3+}$; $M(3) = Fe_{1.00}^{3+}$.

7c. Calculated composition for $Mn_3^{2+}Fe_3^{3+}(OH)_3(H_2O)_7(PO_4)_4$ (see Mrose, 1955).

TABLE IV. *Whiteite and jahnsite. Optical properties*

| | Whiteite (type) | Whiteite (Ca-poor) | Jahnsite (type)* | Jahnsite (Fletcher)† |
|-----------------------------|---|------------------------|--------------------------------------|-------------------------|
| α | 1.580(3) | 1.575(5) | 1.640(3) | 1.682 |
| β | 1.585(3) | 1.585(5) | 1.658(3) | 1.695 |
| γ | 1.590(3) | 1.595(5) | 1.670(3) | 1.707 |
| Sign | + | — | — | —? |
| $2V$ (obs) | 40–50° | 80–90° | large | large |
| $\langle n \rangle$ (calc)‡ | 1.58 | 1.59 | 1.67 | 1.68 |
| Orientation | $\alpha \parallel b$ $\beta \parallel a$ | $\alpha \perp \{001\}$ | γ $\alpha: [001] 18^\circ$ | — |

* Moore (1974).

† Mrose (1955). The calculated mean index is based on analysis 7b in Table III.

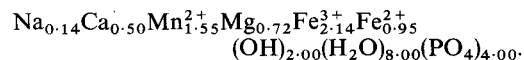
‡ Calculated from the relationship of Gladstone and Dale, the cell contents, and specific gravities.

certain test for the species. Relative sizes of the dominant forms result in a variety of developments, the visual relationships of which are not immediately obvious. Fig. 2 presents several developments commonly found for jahnsites, which supplement the observations of Moore (1974a).

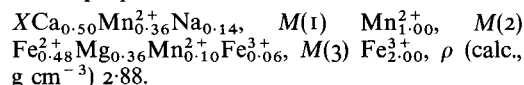
Mrose (1955), in a preliminary note, announced the occurrence of a '... yellow brown mineral occurring as crystals and sheaflike aggregates with rockbridgeite at the Fletcher and Palermo mines, New Hampshire ...' and she suggests that this mineral '... resembles type xanthoxenite more closely than does the previously described xanthoxenite from Palermo'. She proposed the formula $Mn_3^{2+}Fe_3^{3+}(PO_4)_4(OH)_3 \cdot 7H_2O$, although the details of the chemical analysis were not stated. Moore (1974a) alluded to the same material ('golden rockbridgeite' of New England collectors) in his paper.

The results of the powder and single-crystal studies on this material appear in Tables I and II respectively. It is quite clearly a variant of jahnsite group, and Mrose's single-crystal results can be related by noting that the twinned criteria derived from the primitive monoclinic cell closely match her orthogonal cell. Caution was taken to select a split fragment free from twinning; the *hol* and *h1l* precession photographs clearly show the monoclinic aspect of the crystals. Results of an electron-probe analysis averaged from twelve grains appear in Table III under analysis 7a. Owing to the finely admixed nature of the material it was not possible to purify enough grains for wet chemical analysis, and, consequently, oxidation states have to be inferred. Like the whiteite samples from the type locality, the total is low. To derive the formula unit, the calculation was based on $P = 4.00$ such that the sum of the remaining cations leads to complete site occupancy.

We interpret the Fletcher material as a significantly oxidized transition metal-rich jahnsite. The balanced formula is



The proposed distributions of cations are:



It is practically impossible to distinguish among the possibility of vacancies in the $X(r)$ position, the possible presence of hydronium cations, the partial hydroxylation of ligand water to balance charge, and the formal charges of the transition metals without a detailed structure analysis on the same crystals. Thus, the proposed distributions above are a compromise between the available analysis, the structure type, and the greater ease of Fe^{2+} oxidation relative to Mn^{2+} . The good agreement between observed and calculated densities suggests that the above formula is probably a fair chemical

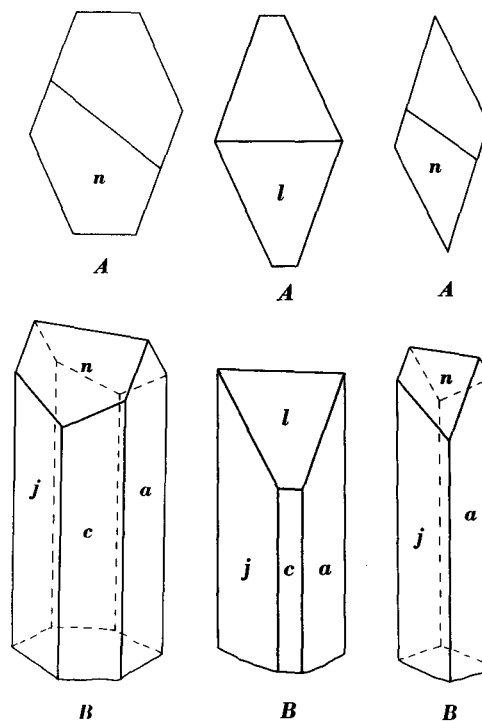


FIG. 2. Crystals of jahnsite showing the forms $c\{001\}$, $a\{100\}$, $j\{201\}$, $l\{011\}$, and $n\{111\}$. A. Plan. B. Clinographic projection (*b*-axis polar). Left: Tip Top pegmatite, South Dakota. Centre: Sapucaia pegmatite, Minas Gerais, Brazil. Right: Palermo No. 1 pegmatite, New Hampshire.

description of Fletcher material. The end-member is jahnsite—(CaMn²⁺Fe²⁺).

It is proposed that the general composition of the jahnsite series be written jahnsite—(XM(1)M(2)) and the whiteite series whiteite—(XM(1)M(2)). Thus, type jahnsite is jahnsite—(CaMn²⁺Mg); the Fletcher material, jahnsite—(CaMn²⁺Fe²⁺); type whiteite and the Yukon samples, whiteite—(CaFe²⁺Mg); and the Ca-poor variant, whiteite—(Mn²⁺Fe²⁺Mg). End-member compositions, adhering to convention, accept the dominant cation at each site.

This classification parallels that for the pumpellyite and julgoldite series proposed by Passaglia and Gottardi (1973) where two kinds of octahedral positions, X (predominantly divalent cations) and Y (predominantly trivalent cations) are involved. The series is split first on the basis of Y populations—Al³⁺ for pumpellyite, Fe³⁺ for julgoldite—and then by the predominant cation in X. Thus, with X = Fe²⁺ and Y = Al³⁺, the nomenclature is pumpellyite—(Fe²⁺). It is appealing to split the series this way since the electrostatic bond strengths for Al³⁺ and Fe³⁺ are considerably greater than those of X-population cations in pumpellyite-julgoldite and the XM(1)M(2) positions and cations in whiteite-jahnsite.

The whiteite-jahnsite series is complicated by the presence of three distinct octahedral positions and uncertainties necessarily arise with regard to site distributions. In principle, chemical composition and refined crystal structure must be known for each crystal in order to assure a reasonably correct assignment of cations over the X, M(1), and M(2) positions. This is clearly a difficult task and we propose that tentative distributions of cations proceed from ionic radii arguments where the radius increases M(3) < M(2) < M(1) < X. Thus, once the composition is known, the contents are calculated on the basis of the formula XM(1)M(2)M(3)₂³⁺(OH)₂(H₂O)₈[PO₄]₄ and the smallest trivalent cations are placed in M(3) until that site is filled, then M(2), etc., until the largest remaining cations are placed in X. It is possible, in oxidized and leached variants, that X may be only partly occupied or empty.

New data on xanthoxenite

A review of xanthoxen and xanthoxenite. Xanthoxenite is an enigmatic species. Originally described by Laubmann and Steinmetz (1920) as *Xanthoxen* from the Hühnerkobel pegmatite, Bavaria, Frondel (1949) resurrected the name for a basic calcium ferric phosphate from the Palermo No. 1 mine, North Groton, New Hampshire. This conclusion was reached, despite inconsistencies between the

original description and his results, on the basis of the identity of a sample labelled 'xanthoxenite' from Hühnerkobel with the Palermo material. A complete wet-chemical analysis on the Palermo material led Frondel (1949) to propose the formula Ca₂Fe³⁺(PO₄)₂(OH)·1½H₂O. Unfortunately, Frondel could not locate the type specimen of Laubmann and Steinmetz. He stated, 'The conclusion thus seems forced that the Palermo material is identical with xanthoxenite, in spite of the discrepancies in the description of the two substances.'

It was impossible to locate any 'xanthoxenite' or 'xanthoxen' sample that unambiguously proved to be the type specimen and we must depend on the descriptive data of Laubmann and Steinmetz (1920). They remarked that the crystals are thin tabular parallel to {010}, monoclinic, the cleavage perfect parallel to {010} and that the mineral is frequently in parallel growth with needles of *Kakoxen* (= cacoxenite). These needles of 'cacoxenite' were observed to extinguish at 8° from the prism axis. This suggests that their 'cacoxenite' is probably strunzite since γ : $[001]$ ranges from 10 to 19° in that mineral according to Frondel (1957), whereas true cacoxenite is hexagonal and would exhibit parallel extinction.

The crucial information rests on fig. 20 of Laubmann and Steinmetz (1920) and the attendant discussion, the former reproduced as fig. 3 in the present investigation. It represents morphological and optical data based on their microscopic study of the type 'xanthoxenite' crystals. Parallel to the plane of the perfect {010} cleavage, the clinodome was observed to make a 41° angle with the outline of the prism. In addition, the γ optic direction provided an acute angle of 36° with the outline of the prism. Mrose (1955) proposed that the yellow-brown material (the jahnsite of the present study) occurring as crystals and sheaf-like aggregates from the Fletcher mine is closer to the material of Laubmann and Steinmetz than the materials of

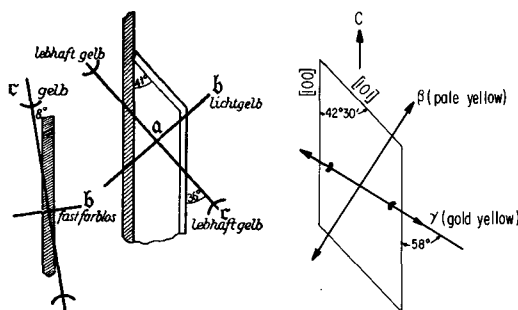


FIG. 3. Optical orientation of the acute bisectrix for stewartites resting on their {010}_m cleavage surfaces. Left: Fig. 20 of Laubmann and Steinmetz (1920). Right: Sketched data of Tennyson (1956).

